

## **Supplementary Information**

### **Genome-wide suppressor screen identifies USP35/USP38 as therapeutic candidates for ciliopathies**

I-Chun Tsai<sup>1</sup>, Kevin A. Adams<sup>1</sup>, Joyce A. Tzeng<sup>1</sup>, Omar Shennib, Perciliz L. Tan<sup>1,2</sup> and Nicholas Katsanis<sup>1, 3, 4, \*</sup>

<sup>1</sup>Center for Human Disease Modeling, Duke University School of Medicine, Durham, NC 27701

<sup>2</sup>Rescindo Therapeutics, Durham, NC 27701

<sup>3</sup>Stanley Manne Children's Research Institute, Ann & Robert H. Lurie Children's Hospital of Chicago, Chicago, IL 60611, USA

<sup>4</sup>Departments of Pediatrics and Cellular and Molecular Biology, Northwestern University Feinberg School of Medicine, Chicago, IL 60611, USA

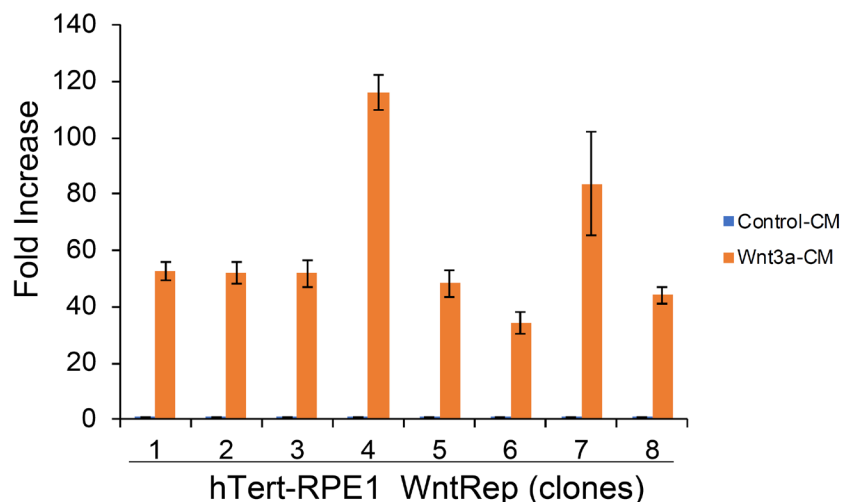
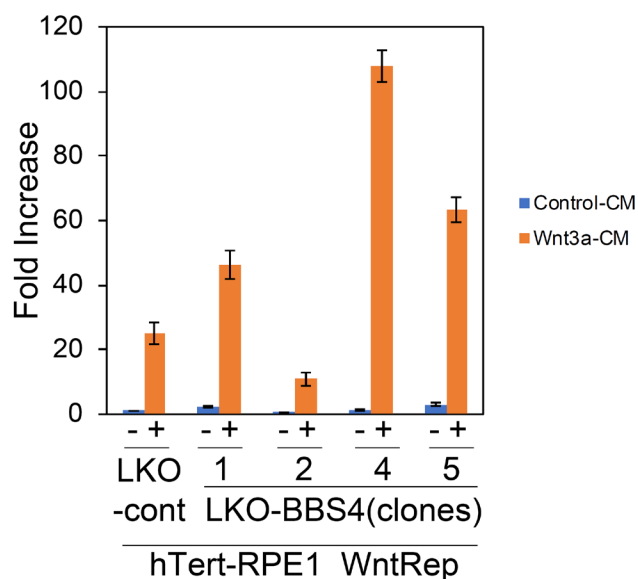
\*Correspondence: Nicholas Katsanis, Ph.D

Stanley Manne Children's Research Institute, Ann & Robert H. Lurie Children's Hospital  
of Chicago

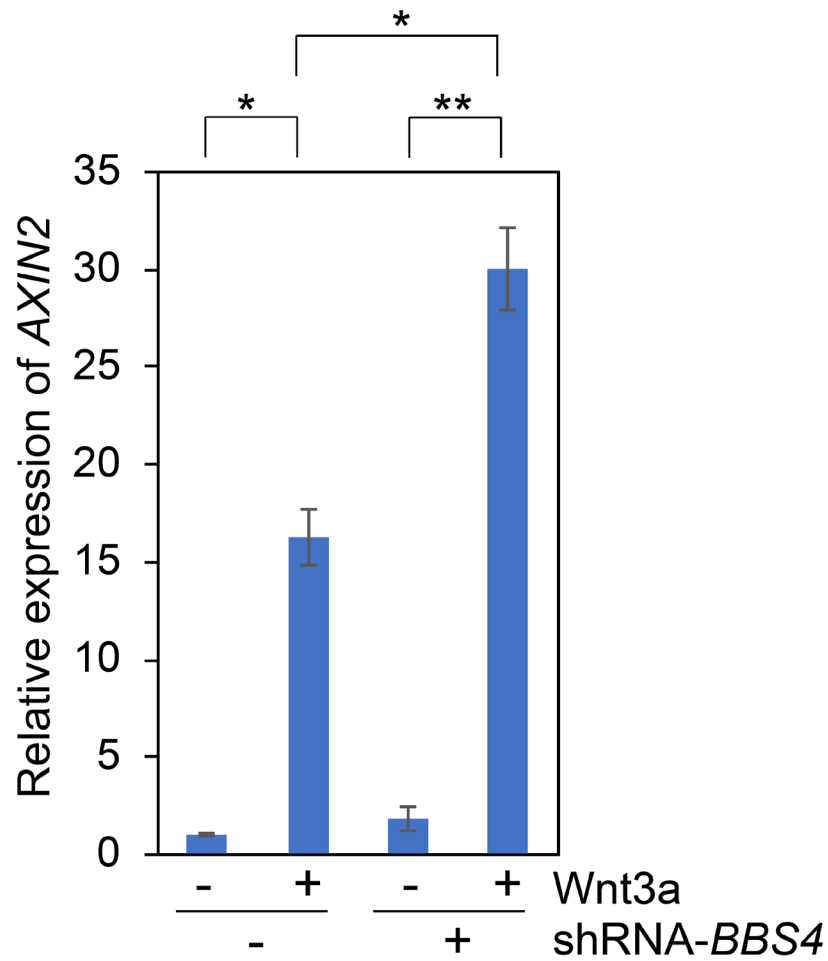
225 E. Chicago Avenue, BOX 205, Chicago, IL 60611

Phone: +1 (312) 503-7263

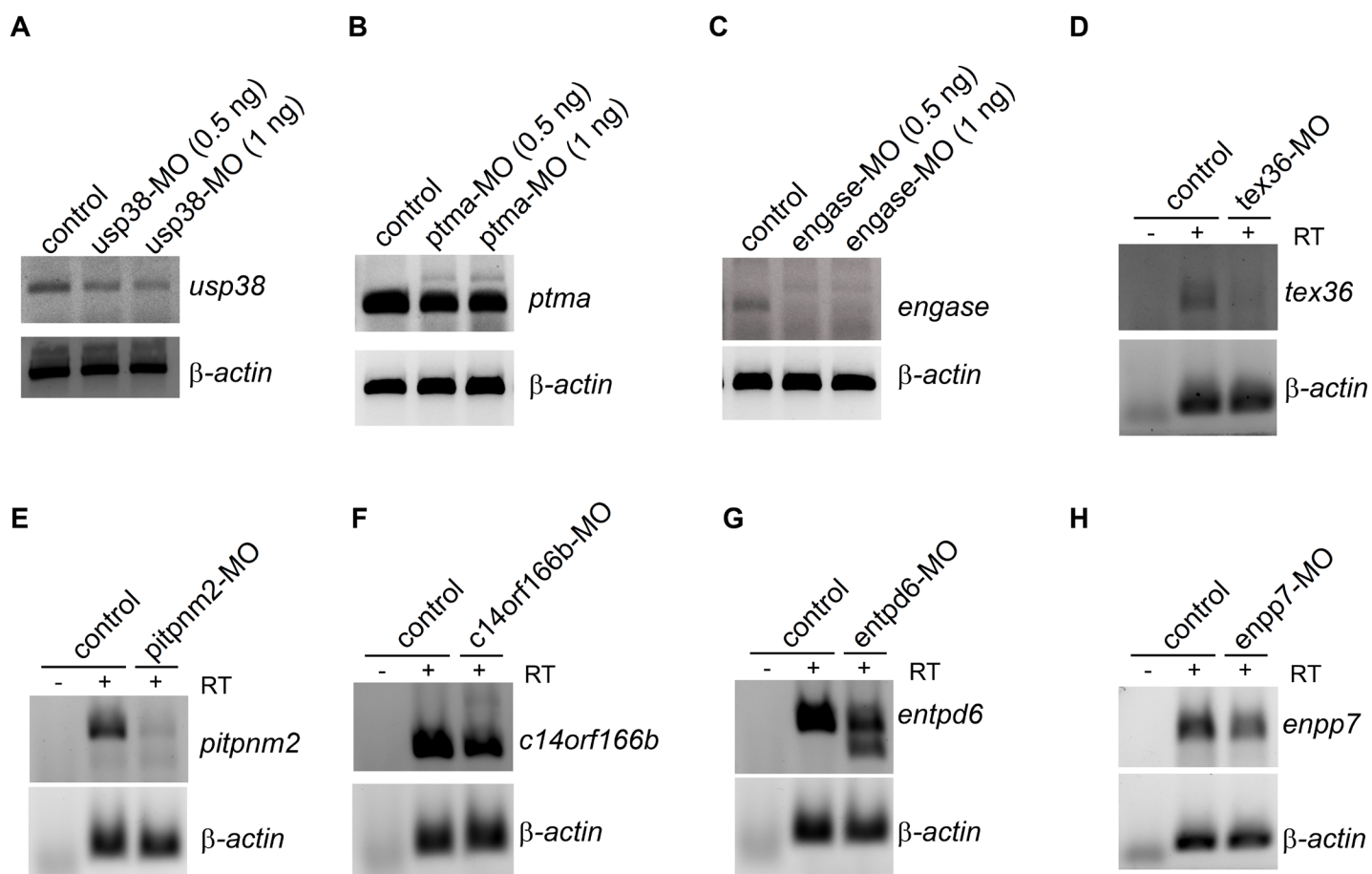
e-mail: [nkatsanis@luriechildrens.org](mailto:nkatsanis@luriechildrens.org)

**A****B****C**

**Supplementary Figure 1 Generation and validation of the hTert-RPE1\_WntRep\_shRNA-BBS4 cell line used for RNAi screen.** (A) hTert-RPE1 cell line was transfected with Wnt Reporter plasmid and selected with Geneticin (500  $\mu$ g/ml) 48 hours post transfection. Eight cell colonies were picked and treated with Control- or Wnt3a-conditioned medium (CM), followed by luciferase assay. Graph represents the fold increase in comparison to Control-CM treatment and error bar indicates the standard deviation of triplicates. Clone 4 were selected for the further generation of BBS4-depleted cell line. (B) hTert-RPE1\_WntRep cell were transduced with LKO-cont (SHC002) or LKO-BBS4 lentivirus, followed by puromycin selection (5  $\mu$ g/ml). Three of control and six of BBS4-depleted cell clones were picked and subjected to Western blot for assessing the suppression of BBS4. HSP90 served as loading control. (C) LKO-control clone 1 and LKO-BBS4 clones 1, 2, 4 and 5 (clone 3 and 6 were dropped due to low viability) from (B) were subjected to Luciferase assay after 8 hours of conditioned media treatment. Graph represents the fold increase in comparison to Control-CM treatment of LKO-cont line and error bar indicates the standard deviation of triplicates. LKO-BBS4 clone 4 were selected for further RNAi screening.

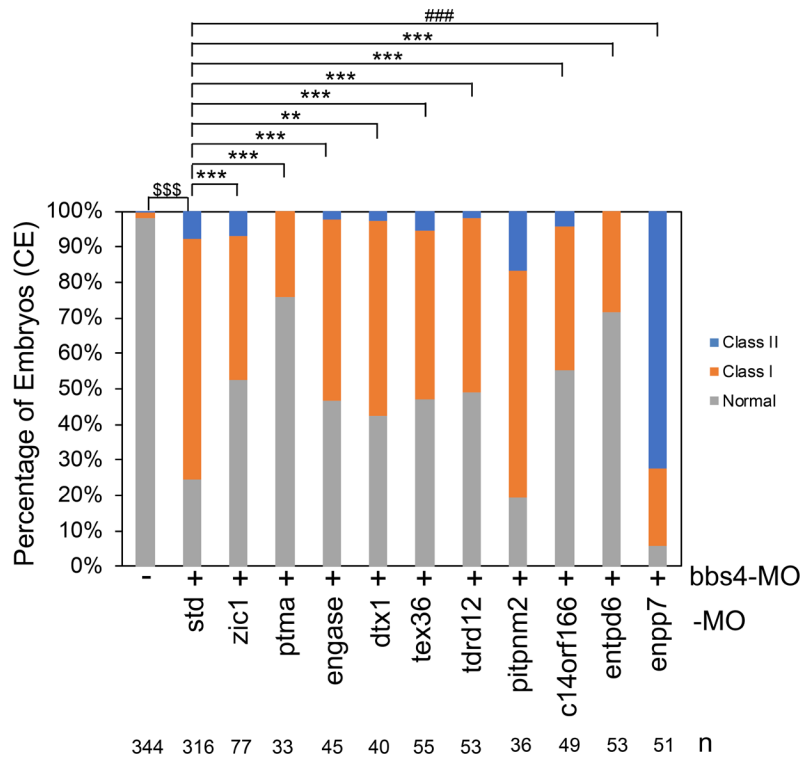


**Supplementary Figure 2 Suppression of *BBS4* enhances the expression of *AXIN2*.** hTert RPE cells which stably express shRNA targeting *BBS4* or non-silencing control were incubated with Wnt3a-conditioned media for 4 hours. The cells were then harvested followed by *AXIN2* qPCR. Compared to the shRNA-control without Wnt3a stimulation, the mean relative expression level of *AXIN2* from triplicated experiments is presented in the graph. Error bar: standard error of mean. Asterisk denotes the significance of *AXIN2* expression (\*:  $p < 0.05$ ; \*\*:  $p < 0.001$ ; 2-tailed t test).

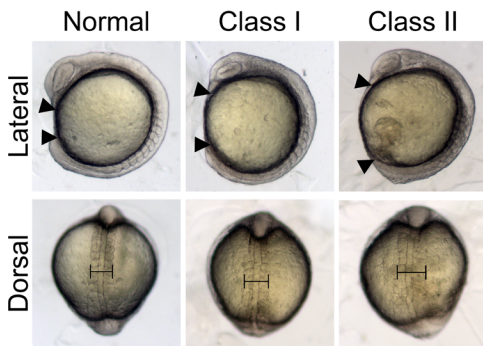


**Supplementary Figure 3 Morpholino knock-down efficiency.** Zebrafish embryos at 1-4 cell stage were injected with the morpholinos targeted to the genes indicated in the figure. 30 hours post of injection, 15 embryos were collected and subjected to RT-PCR for the expression of targeted genes. RT-PCR for  $\beta$ -actin were served as loading control. RT: Reverse Transcriptase.

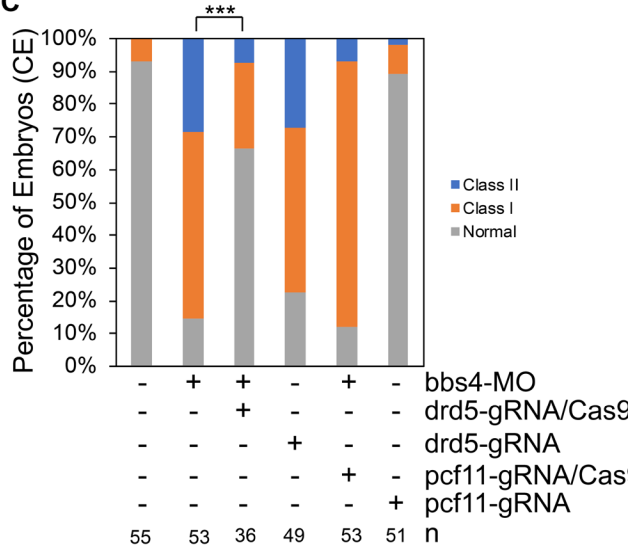
A



B



C

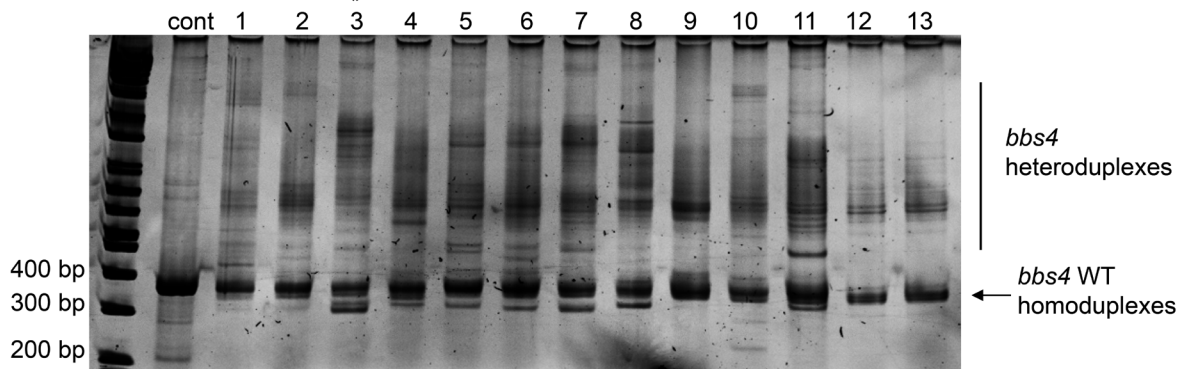


**Supplementary Figure 4 Assessment of the CE rescue by suppression of 13 candidate genes.** (A) zebrafish embryos were injected with *bbs4*-morpholino (*bbs4*-MO) plus either standard control morpholino (std) or the MO targeting to *zic1*, *ptma*, *engase*, *dtx1*, *tex36*, *tdrd12*, *pitpnm2*, *c14orf166*, *entpd6* and *enpp7*. Depletion of *bbs4* results in CE defects, including wider anterior-posterior body gap, somite (Class I) and loss of eyes (Class II) (\$\$\$:  $p < 0.001$  in comparison to control embryos). Co-injection of *zic1*-MO, *ptma*-MO, *engase*-MO, *dtx1*-MO, *tex36*-MO, *tdrd12*-MO, *c14orf166*-MO and *entpd6*-MO in *bbs4* morphants reduces the percentage of both Class I and Class II embryos. (\*\*:  $p < 0.01$ ; \*\*\*:  $p < 0.001$  in comparison to *bbs4* morphant coinjected with std-MO, Chi-square). Co-injection of *enpp7*-MO increases the percentage of both Class I and Class II embryos significantly. (####:  $p < 0.001$  in comparison to *bbs4* morphant co-injected with std-MO). (B) Classification of the embryos with CE defects. CE-deficient embryos exhibit wider anterior-posterior body gap, somite (Class I) and delayed eye development (Class II). (C) *bbs4* morphants were co-injected with gRNA/Cas9 of *drd5* or *pcf11*. Co-injection of *drd5*-gRNA/Cas9 in *bbs4* morphant ameliorates the CE defects (\*\*\*:  $p < 0.001$ , Chi-square).



**A**

ENSDART00000122929 Chr25:2,608,100-2,642,154; ZV9

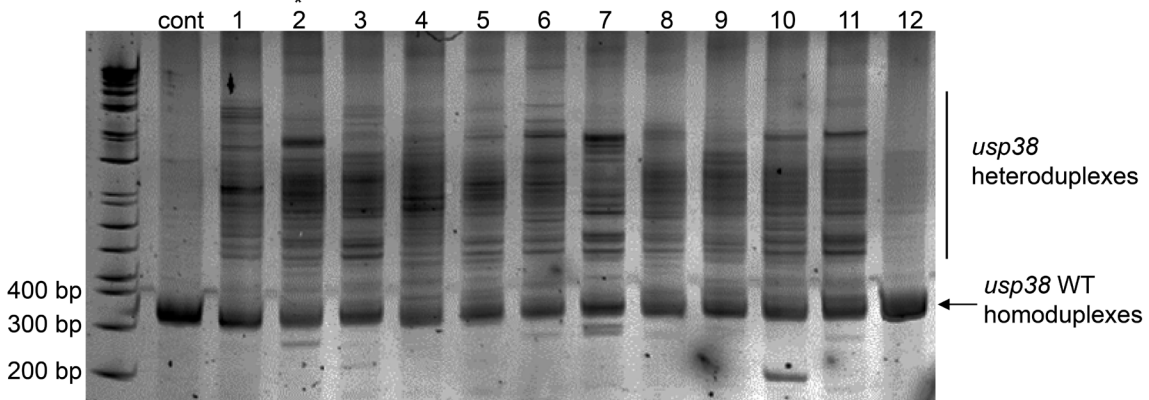
**B****C**

	gRNA target										PAM	
control	atataaagtatataaatatTTTTAAAGTATATATTTTATCTGCAGCTCCTGAGCTTCCC										-a-t---cctggagaaaag	
F0-01	ATATAAAGTATATAAATATTTTTAAAGTATATATTTTATCTGCAGA										---GAGAAGA---A-A---CCTGGAGAGAAG	
F0-02	ATATAC--TATATA-T-T-----CT-C--CT--G-G-----A-----										G-AG--AAG	
F0-03	ATATAAAGTATATAAATATTTTTAAAGTATATATTTTATCTGCAGCTCCTGAGCTTCC										-----GGAGAGAAG	
F0-04	A-----CT-C--CT--G-G-----A-----										G-AGAA--G	
F0-05	ATATAAAGTATATAAATATTTTTAAAGTATATATTTTATCTGCAGCT--T--CT-CC--T--										GGAGAGAAG	
F0-06	ATATAAAGTATATAAATATTTTTAAAGTATATATTTTATCTGCAGCTCCTGAGCTTCCC--T--										GGAGAGAAG	
F0-07	ATATAAAGTATATAAATATTTTTAAAGTATATATTTTATCTGCAGCTCCTGAGCTTCC--T--										GGAGAGAAG	
F0-08	ATATAAAGTATATAAATATTTTTAAAGTATATAC										TTTATCTGCAGCTCCTGAGCT-----GGAGAGAAG	
F0-09	ATATAAAGTATATAAATATTTTTAAAGTATATATTTTATCTGCAGCTCCTGAGCTTCCCTA										ATGTTCTGGAGAGAAG	

**D**

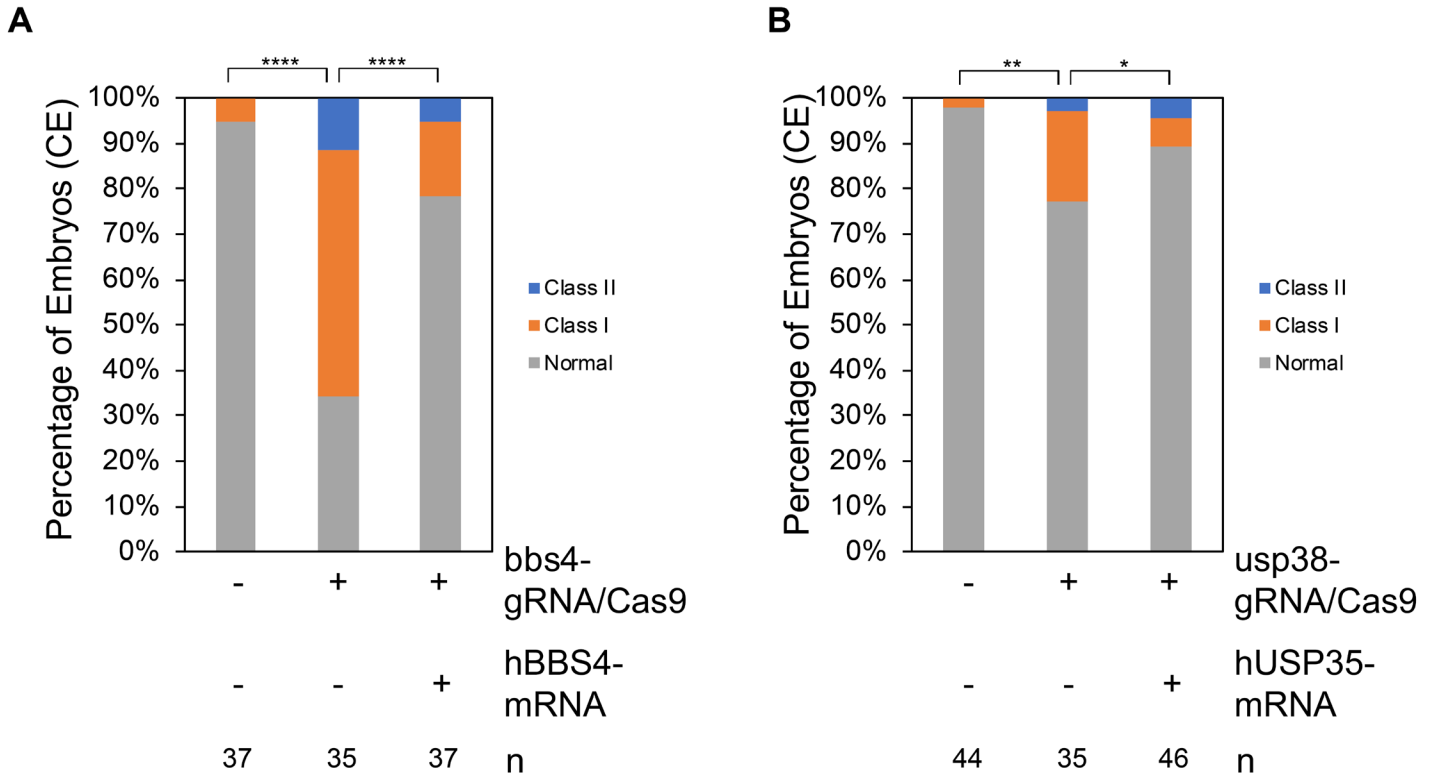
ENSDART00000109678 Chr1:35,183,733-35,196,266; ZV9

usp38 guide RNA

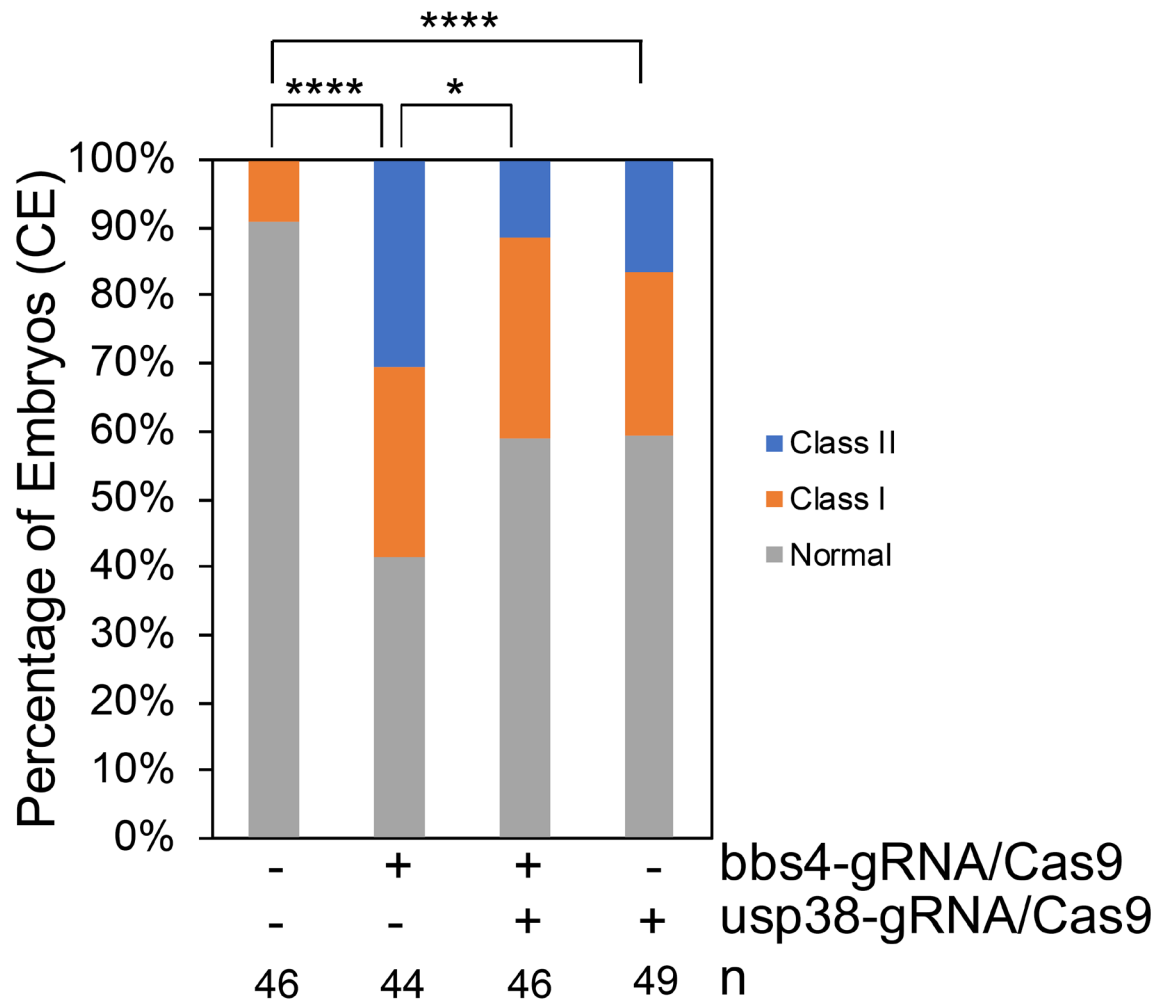
**E****F**

	PAM										gRNA target	
control	ggagcagtgccaggccttgtaccatctcaccacc-gccttattctccagggtgaagatggtttttcagcgtcagat											
F0-01	GGAGCAGTGCCAGG-----GTGAAGATGTTTTTCAGCGTCAGAT											
F0-02	GGAGCAGTGCCAGGCCTTGTACCATCTCACCACC-----TTATTCTCCAGGGTGAAGATGTTTTTCAGCGTCAGAT											
F0-03	GGAGCAGTGCCAGGCCTTGTACCATCTCACCACC-gccttattctccagggtgaagatggtttttcagcgtcagat											
F0-04	GGAGCAGTGCCAGGCCTTGTACCATCTCACCACC-----TTATTCTCCAGGGTGAAGATGTTTTTCAGCGTCAGAT											
F0-05	GGAGCAGTGCCAGGCCTTGTACCATCTCACCACC-gccttattctccagggtgaagatggtttttcagcgtcagat											
F0-06	GGAGCAGTGCCAGGCCTTGTACCATCTCACC-----CCTTATTCTCCAGGGTGAAGATGTTTTTCAGCGTCAGAT											
F0-07	GGAGCAGTGCCAGGCCTTGTACCATCTCACC-----TTATTCTCCAGGGTGAAGATGTTTTTCAGCGTCAGAT											

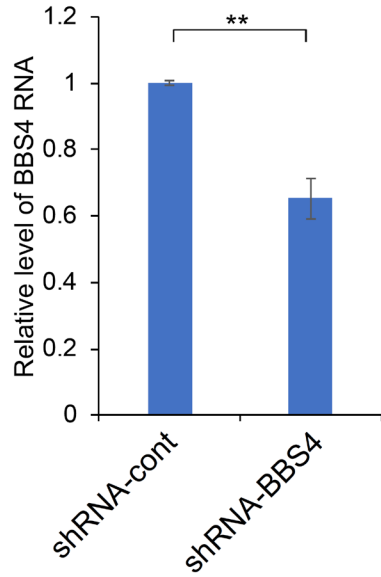
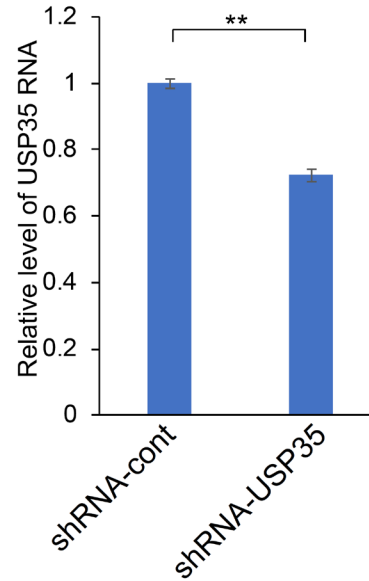
**Supplementary Figure 6 Validation of genome editing efficiency in *bbs4*-CRISPR F0s and *usp38*-CRISPR F0s.** (A) Schematic representation of the zebrafish *bbs4* transcript. yellow boxes: exons; blue box: gRNA targeted site; orange arrowheads: primers for amplifying the potential mutation region. (B) Polyacrylamide gel electrophoresis (20% PAGE) of control and 13 *bbs4*-CRISPR F0 embryos shows the presence of heteroduplexes, indicating targeting events in CRISPR F0s. The PCR products of the embryos annotated with an asterisk (\*) were then cloned into pCR4 for Sanger sequencing. (C) Representative Sanger sequencing results for an un-injected control embryo and 7 randomly selected clones of F0 embryo (\*) injected with *bbs4* gRNA/Cas9 show insertion and or deletion events in the target region. The protospacer adjacent motif (PAM) sequence for gRNA is shown with a pink box and gRNA target region is shown within the blue box. (D) Schematic representation of the zebrafish *usp38* transcript. Red boxes: exons; blue box: gRNA targeted site; orange arrowheads: primers for amplifying the potential mutation region. (E) Polyacrylamide gel electrophoresis (20% PAGE) of control and 12 *usp38*-CRISPR F0 embryos shows the presence of heteroduplexes, indicating targeting events in CRISPR F0s. The PCR products of the embryo annotated with an asterisk (\*) were then cloned into pCR4 for Sanger sequencing. (F) Representative Sanger sequencing results for an un-injected control embryo and 9 randomly selected clones of F0 embryo (\*) injected with *usp38* gRNA/Cas9 show insertion and or deletion events in the target region. The protospacer adjacent motif (PAM) sequence for gRNA is shown in pink box and gRNA target region is shown in blue box.



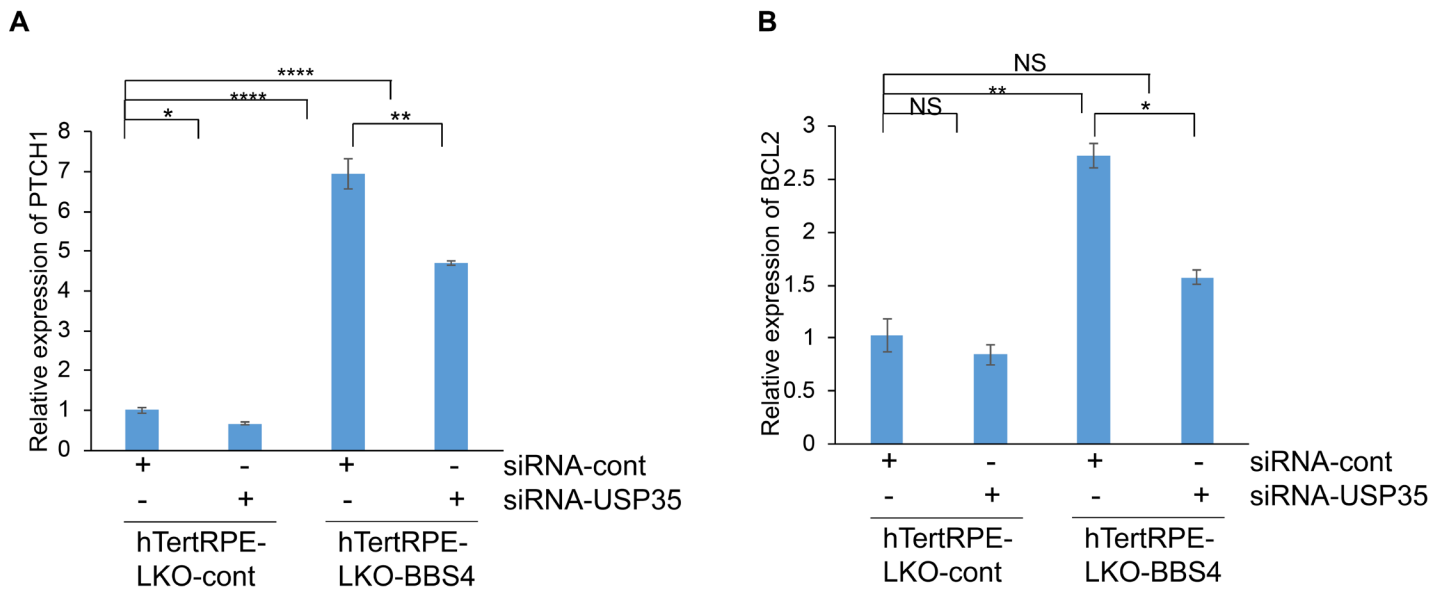
**Supplementary Figure 7 Specificity of *bbs4*- and *usp38*-CRISPR.** (A) 1-cell stage embryos were injected *bbs4*-gRNA/Cas9 with or without human BBS4 mRNA. The embryos were then scored for CE phenotype at 8-10 somite stage. While *bbs4*-gRNA/Cas9 leads to CE defects, co-injection of human BBS4 mRNA rescues the CE defect caused by *bbs4* depletion. \*\*\*\*:  $p < 0.0001$  (Chi-square). (B) 1-cell stage embryos were injected *usp38*-gRNA/Cas9 with or without human USP35 mRNA. The embryos were then scored for CE phenotype at 8-10 somite stage. While *usp38*-gRNA/Cas9 leads to CE defects, co-injection of human USP35 mRNA rescues the CE defect caused by USP38 depletion. \*\*:  $p < 0.01$ , \*:  $p < 0.05$  (Chi-square).



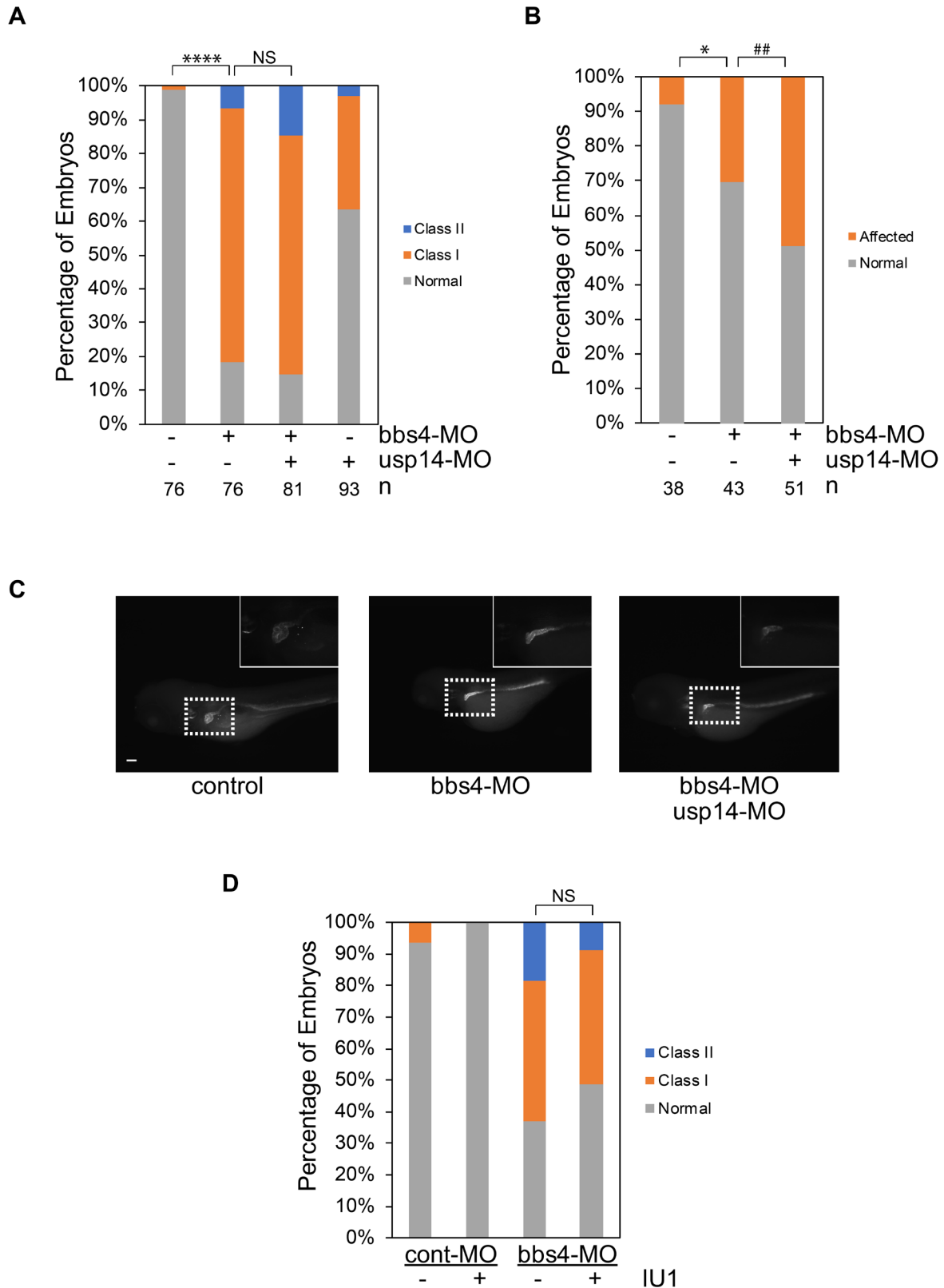
**Supplementary Figure 8 Depletion of *usp38* rescues the CE defects in *bbs4*-CRISPR F0 embryos.** Similar to *bbs4* morphants, *bbs4* F0 mutant embryos also display deficient CE development. Co-injection of *usp38*-gRNA/Cas9 can rescue this defect. \*:  $p < 0.05$ , \*\*\*\*:  $p < 0.0001$  (Chi-square).

**A****B**

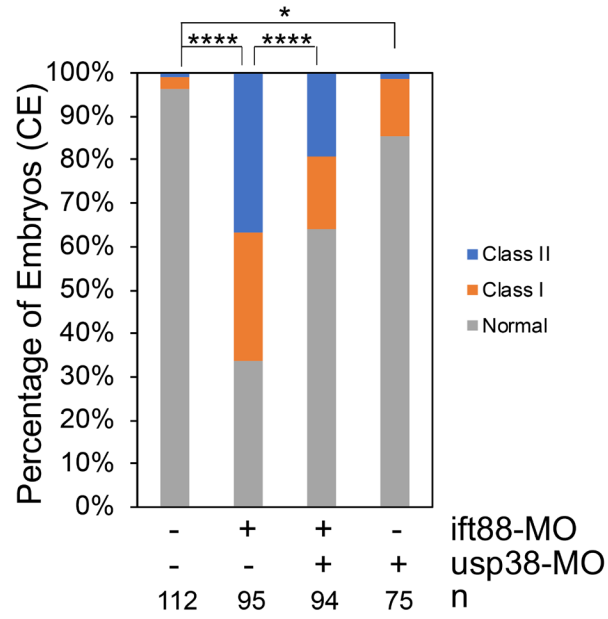
**Supplementary Figure 9 shRNA-mediated *BBS4* and *USP35* suppression in HEK293 cells.** (A) HEK293 cells were transfected with shRNA-cont or shRNA-*BBS4* constructs. 72 hours post transfection, the cells were harvested followed by *BBS4* qRT-PCR.  $p < 0.001$  (2-tailed t test) (B) HEK293 cells were transfected with shRNA-cont or shRNA-*USP35* constructs. 72 hours post transfection, the cells were harvested followed by *USP35* qRT-PCR. \*\*:  $p < 0.001$  (2-tailed t test).



**Supplementary Figure 10 *USP35* suppression ameliorate the hyperactivation of HH signaling caused by depletion of *BBS4*.** hTert RPE cells which stably express shRNA targeting *BBS4* or non-silencing control were transfected with siRNA-control or siRNA-*USP35*. 72 hours post transfection, the cells were harvested followed by (A) *USP35* qRT-PCR, (B) *PTCH1* qRT-PCR and (C) *BCL2* qRT-PCR. Compared to the shRNA-control, the mean relative expression level of *PTCH1* and *BCL2* from triplicated experiments is presented in the graph. Error bar: standard error of mean. Asterisk denotes the significance of *PTCH1* and *BCL2* expression (\*:  $p < 0.05$ ; \*\*:  $p < 0.001$ , \*\*\*\*:  $p < 0.0001$  and NS: non-significant; 2-tailed t test).



**Supplementary Figure 11 Knockdown of *usp14* does not lead to the amelioration of the defects seen in *bbs4* morphants.** (A) Co-injection of *usp14*-MO does not rescue the CE defects seen in *bbs4* morphants. \*\*\*\*:  $p < 0.0001$ ; NS: non-significant. (Chi-square). (B) Unlike *usp38* suppression, knockdown of *usp14* does not rescue the atrophy and convolution deficit seen in *bbs4* morphants. \*:  $p < 0,05$ ; ##:  $p < 0.01$  but worse CE defect. (Chi-square). (C) Representative images of *bbs4* morphant and *bbs4/usp14* morphant. (D) Treatment of IU1 (1  $\mu$ M) does not ameliorate the CE defects in *bbs4* morphant.



**Supplementary Figure 12 Suppression of *usp38* rescues the CE defects in *ift88* morphant.** Similar to *bbs4* morphants, *ift88* morphant also display deficient CE development. Co-injection of *usp38*-morpholino can rescue this defect. \*:  $p < 0.05$ , \*\*\*\*:  $p < 0.0001$ . (Chi-square).

Gene Symbol	Full Name	Physiological Roles	References
DTX1	deltex E3 ubiquitin ligase 1	1. Notch signaling 2. Transcriptional factor	(1, 2)
PITPNM2	phosphatidylinositol transfer protein, membrane-associated 2	Membrane-associated phosphatidylinositol transfer domain-containing protein that shares homology with the <i>Drosophila</i> retinal degeneration B (rdgB) protein	(3)
RHOXF1	Rhox homeobox family, member 1	Likely a transcription factor that may play a role in reproduction	(4)
DRD5	dopamine receptor D5	This gene encodes the D5 subtype of the dopamine receptor, which is a G-protein coupled receptor and stimulates adenylyl cyclase.	(5)
ENTPD6	ectonucleoside triphosphate diphosphohydrolase 6 (putative function)	mediate catabolism of extracellular nucleotides	(6)
C14orf166B (LRRC74A)	leucine rich repeat containing 74A	not clear	
PCF11	PCF11 cleavage and polyadenylation factor subunit	1. Pol II transcription termination 2. degradation of the 3' product of polyA site cleavage	(7, 8)
TEX36	testis expressed 36	not clear	
ZIC1	Zic family member 1	1. C2H2-type zinc finger protein 2. Transcriptional factor	(9)
PTMA	prothymosin, alpha	1. Oncoprotein 2. Regulate apoptosis	(10, 11)
ENGASE	endo-beta-N-acetylglucosaminidase	Catalyzes the hydrolysis of peptides and proteins with mannose modifications	(12)
ENPP7	ectonucleotide pyrophosphatase/phosphodiesterase 7	1. Converts sphingomyelin to ceramide and phosphocholine 2. Protect the intestinal mucosa from inflammation and tumorigenesis	(13, 14)
TDRD12	tudor domain containing 12	Essential for piRNA biogenesis and transposon silencing (24067652)	(15)
USP35	ubiquitin specific peptidase 35	1. Catalyze the removal of ubiquitin from other proteins 2. Regulate PARK2-mediated mitophagy 3. Regulate cell cycle progression	(16, 17)

**Supplementary Table 1 Background of the validated hits of Genome-wide siRNA screening.**

USP Genes	Z-score (Plate A)	Z-score (Plate B)	p-value
USP1	1.33760963	-0.4820841	0.533
USP2	10.66938818	-5.070544895	0.523
USP3	4.679920856	2.554573449	0.853
USP4	-2.290356334	0.042842651	0.270
USP5	12.80878333	3.515914152	0.967
USP6	3.946325591	-0.691606989	0.798
USP7	-3.68335684	-4.65143579	0.025
USP8	-3.248171881	-3.734303129	0.046
USP9X	19.91255687	-1.050123802	0.936
USP9Y	-2.70683676	-3.167713816	0.083
USP10	2.471217499	3.685649796	0.736
USP11	-1.547728841	2.072648801	0.545
USP12	6.239118983	4.216985548	0.897
USP13	0.604915299	-0.870610858	0.544
USP14	-2.192564453	0.856050536	0.415
USP15	-2.749048088	16.41464922	0.737
USP16	18.40737356	-2.469127551	0.844
USP17	0.976633913	-5.711985388	0.164
USP18	-2.439943595	2.125504442	0.550
USP19	-1.048583607	-2.408568463	0.245
USP20	-2.87066469	36.96059398	0.713
USP21	-1.532362871	-3.28695565	0.193
USP22	-1.290959562	4.949977457	0.771
USP24	2.578753762	0.937717442	0.743
USP25	3.90958472	10.73151554	0.877
USP26	0.261393387	10.43685132	0.946
USP27X	-3.100789787	-1.389550456	0.168
USP28	4.65843565	1.237332422	0.528
USP29	9.440091626	-4.896432085	0.299
USP30	-3.040434023	-3.450217625	0.111
USP31	-2.938211963	-4.629404933	0.066
USP32	-2.274049531	-2.757646045	0.120
USP33	-0.00219397	-0.959265881	0.454
USP34	-0.478202685	-4.2326098	0.370
USP35	-3.358294984	-7.793328783	0.040
USP36	-3.289820547	0.28404334	0.341
USP37	12.73675312	16.05156306	0.978
USP38	-2.054058659	-5.716617074	0.141
USP39	7.05586132	7.05586132	0.368
USP40	4.162519225	13.2079016	0.917
USP41	-1.082098421	12.23317773	0.834
USP42	-0.496379532	-6.219526835	0.321
USP43	-1.478149443	-1.752396598	0.199
USP44	-3.960665354	-3.545667845	0.048
USP45	-4.661926926	0.561916585	0.676
USP46	0.91801109	0.508821842	0.585
USP47	-1.006393824	2.942729397	0.597
USP48	-0.669890215	-3.213993901	0.332
USP49	5.028920654	5.628313774	0.738
USP50	29.74047116	1.001561841	0.924
USP51	10.95921781	-3.88994719	0.595
USP52	-5.71135241	-4.240053701	0.185
USP53	3.944671103	2.506637632	0.728

**Supplementary Table 2 Genome-wide siRNA screening results of known USP genes.**

Name	Sequence (5'- 3')
hAxin2_F	AGGTTCTGGCTATGTCTTTGC
hAxin2_R	TCTGGAGCTGTTTCTTACTGC
hUSP35_F	ATCTGTCAGCAACGTCACC
hUSP35_R	CCTTCATCCTCATCCTTGTCTTC
hUSP38_F	CGACTTTGGTTTCCTCTTGTG
hUSP38_R	CTTCTCTTCACTGGGCTTAGG
hBCL2_F	GTGGATGACTGAGTACCTGAAC
hBCL2_R	CCTGCAGCTTTGTTTCATGG
hPTCH1_F	GGCCCTTGTTTTGAATGGTG
hPTCH1_R	TTGAGTGGAGTTCTGTGCG
zUSP38_F	ACCTCTACGACAGCATTCTTG
zUSP38_R	CTGTTTCTGATTTGCCTGTGATC

**Supplementary Table 3 qRT-PCR primer sequence.** h: human; z: zebrafish.

## References

1. Mukherjee A, Veraksa A, Bauer A, Rosse C, Camonis J, and Artavanis-Tsakonas S. Regulation of Notch signalling by non-visual beta-arrestin. *Nat Cell Biol.* 2005;7(12):1191-201.
2. Zheng L, and Conner SD. PI5P4Kgamma functions in DTX1-mediated Notch signaling. *Proc Natl Acad Sci U S A.* 2018;115(9):E1983-E90.
3. Lev S, Hernandez J, Martinez R, Chen A, Plowman G, and Schlessinger J. Identification of a novel family of targets of PYK2 related to Drosophila retinal degeneration B (rdgB) protein. *Mol Cell Biol.* 1999;19(3):2278-88.
4. Borgmann J, Tuttelmann F, Dworniczak B, Ropke A, Song HW, Kliesch S, et al. The human RHOX gene cluster: target genes and functional analysis of gene variants in infertile men. *Hum Mol Genet.* 2016;25(22):4898-910.
5. Yu P, Sun M, Villar VA, Zhang Y, Weinman EJ, Felder RA, et al. Differential dopamine receptor subtype regulation of adenylyl cyclases in lipid rafts in human embryonic kidney and renal proximal tubule cells. *Cell Signal.* 2014;26(11):2521-9.
6. Ivanenkov VV, Murphy-Piedmonte DM, and Kirley TL. Bacterial expression, characterization, and disulfide bond determination of soluble human NTPDase6 (CD39L2) nucleotidase: implications for structure and function. *Biochemistry.* 2003;42(40):11726-35.
7. West S, and Proudfoot NJ. Human Pcf11 enhances degradation of RNA polymerase II-associated nascent RNA and transcriptional termination. *Nucleic Acids Res.* 2008;36(3):905-14.
8. Zhang Z, Klatt A, Henderson AJ, and Gilmour DS. Transcription termination factor Pcf11 limits the processivity of Pol II on an HIV provirus to repress gene expression. *Genes Dev.* 2007;21(13):1609-14.
9. Bagutti C, Forro G, Ferralli J, Rubin B, and Chiquet-Ehrismann R. The intracellular domain of teneurin-2 has a nuclear function and represses zic-1-mediated transcription. *J Cell Sci.* 2003;116(Pt 14):2957-66.
10. Jiang X, Kim HE, Shu H, Zhao Y, Zhang H, Kofron J, et al. Distinctive roles of PHAP proteins and prothymosin-alpha in a death regulatory pathway. *Science.* 2003;299(5604):223-6.
11. Tsai YS, Jou YC, Tsai HT, Shiau AL, Wu CL, and Tzai TS. Prothymosin-alpha enhances phosphatase and tensin homolog expression and binds with tripartite motif-containing protein 21 to regulate Kelch-like ECH-associated protein 1/nuclear factor erythroid 2-related factor 2 signaling in human bladder cancer. *Cancer Sci.* 2019;110(4):1208-19.
12. Suzuki T, Yano K, Sugimoto S, Kitajima K, Lennarz WJ, Inoue S, et al. Endo-beta-N-acetylglucosaminidase, an enzyme involved in processing of free oligosaccharides in the cytosol. *Proc Natl Acad Sci U S A.* 2002;99(15):9691-6.
13. Wu J, Hansen GH, Nilsson A, and Duan RD. Functional studies of human intestinal alkaline sphingomyelinase by deglycosylation and mutagenesis. *Biochem J.* 2005;386(Pt 1):153-60.
14. Wu J, Nilsson A, Jonsson BA, Stenstad H, Agace W, Cheng Y, et al. Intestinal alkaline sphingomyelinase hydrolyses and inactivates platelet-activating factor by a phospholipase C activity. *Biochem J.* 2006;394(Pt 1):299-308.
15. Pandey RR, Tokuzawa Y, Yang Z, Hayashi E, Ichisaka T, Kajita S, et al. Tudor domain containing 12 (TDRD12) is essential for secondary PIWI interacting RNA biogenesis in mice. *Proc Natl Acad Sci U S A.* 2013;110(41):16492-7.
16. Park J, Kwon MS, Kim EE, Lee H, and Song EJ. USP35 regulates mitotic progression by modulating the stability of Aurora B. *Nat Commun.* 2018;9(1):688.
17. Wang Y, Serricchio M, Jauregui M, Shanbhag R, Stoltz T, Di Paolo CT, et al. Deubiquitinating enzymes regulate PARK2-mediated mitophagy. *Autophagy.* 2015;11(4):595-606.